Unified description of lepton- and hadron-induced reactions

V. Batozskaya[a*], L. Jenkovszky[b,c†], A. Salii[b‡]
[a] *Joint Institute for Nuclear Research*
141980, Dubna, Russia
[b] *Bogolyubov Institute for Theoretical Physics*
National Academy of Sciences of Ukraine, UA-03680 Kiev, Ukraine
[c] *Wigner Research Centre for Physics, Hungarian Academy of Sciences*
1525 Budapest, POB 49, Hungary

Abstract

We extend a simple Pomeron pole amplitude by t and $Q^2,\ M_V$ dependencies inspired by geometrical ideas. The experimentally transition from *soft* to *hard* dynamics is realized by the introduction of two Pomeron poles with different $Q^2,\ M_V-$ dependent residue. A unified description of deeply virtual Compton scattering as well as the elastic electroproduction of all vector meson is suggested.

1 Introduction

The forward slope of the the differential cross sections for elastic scattering is known to be related to the masses/virtualities of the interacting particles. This phenomenon is evident e.g. from Fig.1, where the forward slope $B(\tilde{Q}^2) = \frac{d}{dt}\ln\frac{d\sigma}{dt}$ is plotted against the the variable $\tilde{Q}^2 = Q^2 + M_V^2$[1].

The slope is proportional to the *interaction radius* $R(\tilde{Q}^2)$, which decreases with increasing of $\tilde{Q}^2$ until it reaches saturation value (about $4.5\,GeV^{-2}$), that correspond to the mass of the nucleon in the lower vertex (Fig.2). In this *geometrical* picture, the largest slope (radius) is expected for real Compton scattering $\tilde{Q}^2 = 0$, which may require a separate treatment. In the present paper we deal with exclusive electroproduction of real photons (**DVCS**), vector mesons production (**VMP**) as well as elastic proton-proton scattering, using the above *geometrical* considerations and writing the scattering amplitude in the form:

$$A(s,t,M_V^2) \sim e^{B(s,M_V^2)t}, \tag{1}$$

where $B(M^2) \sim 1/f(M_V^2)$. This approach was used in Ref. [1] for the simpler case of photoproduction, $\tilde{Q}^2 = 0$, excluding real Compton scattering, and without considering nucleon scattering, to be also included below.

While the geometrical considerations proved to be efficient for photoproduction [1], they are not sufficient in the case of electroproduction $Q^2 = 0$, since the relevant cross sections will increase with $\tilde{Q}^2$ contradicting the experimental data. To remedy this deficiency, the rise must

*e-mail: varvara.batozskaya@cern.ch
†e-mail: jenk@bitp.kiev.ua
‡e-mail: saliy.andriy@gmail.com

[1] The use of the variable $\tilde{Q}^2 = (M_V^2 + Q^2)$ implies symmetry between the mass M_V^2 and virtuality Q^2, which should imply equal slopes (radii) for e.g. J/ψ production near $Q^2 = 0$ and ρ electroproduction near $Q^2 \approx 9$ GeV^2, which is not quite the case.

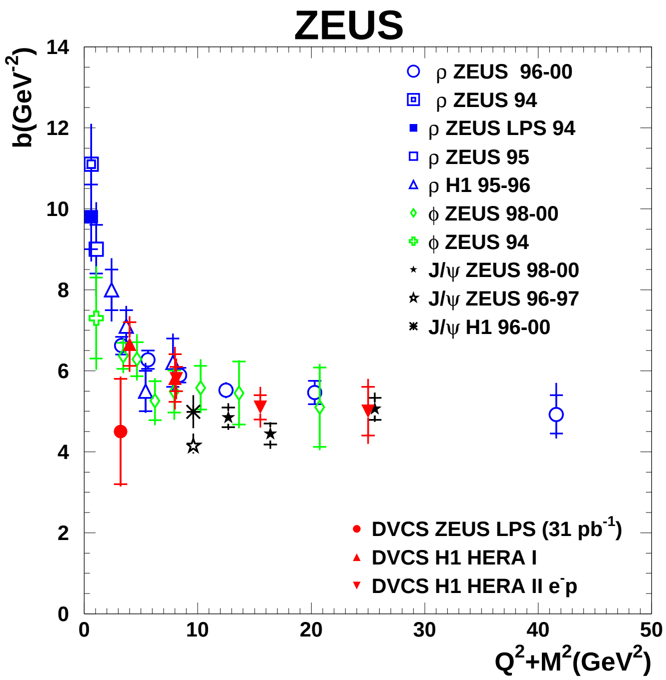

Figure 1: The $B-$slope as a function of $\tilde{Q}^2 = Q^2 + M^2$. Compilation of data for various VMP and DVCS processes measured at ZEUS (see [2]).

be compensated by multiplying the amplitude by a function that decreases with $\tilde{Q}^2$. Moreover, to cope with the observed trend of *hardening* the dynamics as $\tilde{Q}^2$ increases, and following Refs. [3, 4], we introduce two components for the diffractive (Pomeron) amplitude of the type Eq. (1), soft A_s and hard A_h, each one to be multiplied by a relevant $\tilde{Q}^2-$dependent factor $H_i(\tilde{Q}^2),\ i = s, h$. These factors should be chosen in a way to provide increasing of the hard component weight with increasing of Q^2. To avoid conflict with unitarity, the rise with $\tilde{Q}^2$ of the hard component is finite, and it terminates at some *saturation* scale $\tilde{Q}^2_s$ whose value will be determined phenomenologically. Explicit examples of these functions will be given below.

Recently a model for exclusive production of vector particles at HERA was suggested and successfully fitted to the HERA data [1, 5, 6]. In that model, the interplay between t and $\tilde{Q}^2$ is achieved by introducing a new variable $z = t - \tilde{Q}^2$. Good fits were obtained at those papers, however only at the cost of fitting each reaction separately.

This paper is organized as follows: in Sec. 2.1 the Reggeometryical model and the functions $H(\tilde{Q}^2)$ are introduced. In Sec. 2.2 Model with two Pomeron components: "soft" and "hard" are presented. In Sec. 2.3 the results of the fit are presented. For the moment we present the

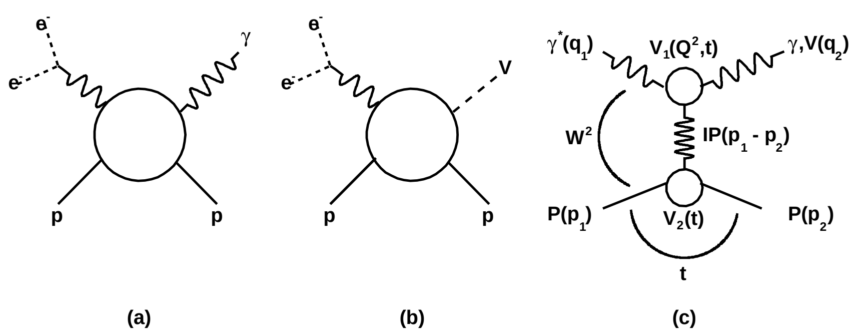

Figure 2: Diagrams of DVCS (a) and VMP (b); (c) DVCS (VMP) amplitude in a Regge-factorized form.

fit with one term, but in the future we expect using Pomeron with two components. In our calculations we start with a simple linear Pomeron trajectory, to be replaced by a more advance logarithmic one.

2 Models and fitting strategy

2.1 The model

$$A(s,t,M,Q^2) = \xi(t)\beta(t,M,Q^2)(s/s_0)^{\alpha(t)}, \tag{2}$$

where $\xi(t) = e^{-i\pi\alpha(t)}$ is the signature factor and $\beta(t,M,Q^2)$ is the residue factor to be specified as

$$\beta(t,M,Q^2) = \exp\Big[2\Big(\frac{a}{M_V^2+Q^2} + \frac{b}{2m_N^2}\Big)t\Big]. \tag{3}$$

$$A(s,t,M,Q^2) = \tilde{A}_0\xi(t)(s/s_0)^{\alpha(t)}e^{-2\left(\frac{a}{M_V^2+Q^2}+\frac{b}{2m_N^2}\right)|t|}. \tag{4}$$

$$\frac{d\sigma}{d|t|} = \frac{\pi}{s^2}|A(s,t,M,Q^2)|^2 = A_0(s/s_0)^{2(\alpha_0-1-\alpha'|t|)}e^{-4\left(\frac{a}{M_V^2+Q^2}+\frac{b}{2m_N^2}\right)|t|}. \tag{5}$$

$$\frac{d\sigma}{d|t|} = A_0(s/s_0)^{2(\alpha_0-1)}e^{-\left[2\alpha'\ln(s/s_0)+4\left(\frac{a}{M_V^2+Q^2}+\frac{b}{2m_N^2}\right)\right]|t|} = Ce^{-B|t|}. \tag{6}$$

$$B(s,\tilde{Q}^2) = \frac{d}{dt}\ln\frac{d\sigma}{d|t|} = 2\alpha'\ln(s/s_0) + 4\Big(\frac{a}{M_V^2+Q^2} + \frac{b}{2m_N^2}\Big). \tag{7}$$

$$\sigma_{el} = \frac{1}{B}\frac{d\sigma}{dt}\Big|_{t=0} = \frac{C}{B}. \tag{8}$$

$$\sigma_{el} = \frac{A_0(s/s_0)^{2(\alpha_0-1)}}{2\alpha'\ln(s/s_0)+4\left(\frac{a}{M_V^2+Q^2}+\frac{b}{2m_N^2}\right)}. \tag{9}$$

In the case $a>0$ when $\tilde{Q}^2 = M_V^2 + Q^2$ grows $B(s,\tilde{Q}^2)$ falls, but $\frac{d\sigma}{d|t|}$ and σ_{el} become larger. While the behavior of $B(s,\tilde{Q}^2)$ is conistent with the experimental data, the behavior of $\frac{d\sigma}{d|t|}$ and σ_{el} are not.

2.2 Reggeometry with Hard and Soft pomerons

We build the scattering amplitude that contain two terms soft and hard with two different $\widetilde{Q^2}$-dependent factors:

$$A(s,t,Q^2,{M_v}^2) = \frac{\tilde{A}_s}{\left(1+\frac{\widetilde{Q^2}}{\widetilde{Q_s^2}}\right)^{n_s}}e^{-i\frac{\pi}{2}\alpha_s(t)}\left(\frac{s}{s_{0s}}\right)^{\alpha_s(t)}e^{2\left(\frac{a_s}{\widetilde{Q^2}}+\frac{b_s}{2m_p^2}\right)t} \tag{10}$$

$$+\frac{\tilde{A}_h\left(\frac{\widetilde{Q^2}}{\widetilde{Q_h^2}}\right)}{\left(1+\frac{\widetilde{Q^2}}{\widetilde{Q_h^2}}\right)^{n_h+1}}e^{-i\frac{\pi}{2}\alpha_h(t)}\left(\frac{s}{s_{0h}}\right)^{\alpha_h(t)}e^{2\left(\frac{a_h}{\widetilde{Q^2}}+\frac{b_h}{2m_p^2}\right)t}.$$

Then it's possible to calculate integrated and differential elastic cross sections:

$$\frac{d\sigma_{el}}{d|t|} = H_s^2 e^{2\{L_s(\alpha_s(t)-1)+\mathfrak{g}_s t\}} + H_h^2 e^{2\{L_h(\alpha_h(t)-1)+\mathfrak{g}_h t\}} \tag{11}$$

$$+2H_sH_he^{\{L_s(\alpha_s(t)-1)+L_h(\alpha_h(t)-1)+(\mathfrak{g}_{\mathfrak{s}}+\mathfrak{g}_{\mathfrak{h}})t\}}\cos\left(\frac{\pi}{2}(\alpha_s(t)-\alpha_h(t))\right),$$

$$\sigma_{el}=\frac{H_s^2e^{2\{L_s(\alpha_{0s}-1)\}}}{2(\alpha'_sL_s+\mathfrak{g}_{\mathfrak{s}})}+\frac{H_h^2e^{2\{L_h(\alpha_{0h}-1)\}}}{2(\alpha'_hL_h+\mathfrak{g}_{\mathfrak{h}})}+2H_sH_he^{L_s(\alpha_{0s}-1)+L_h(\alpha_{0h}-1)}\frac{\mathfrak{B}\cos\phi_0+\mathfrak{L}\sin\phi_0}{\mathfrak{B}^2+\mathfrak{L}^2},\quad(12)$$

where: $H_s=\frac{A_s}{\left(1+\frac{\widetilde{Q^2}}{Q_s^2}\right)^{n_s}},\quad H_h=\frac{A_h\left(\frac{\widetilde{Q^2}}{Q_h^2}\right)}{\left(1+\frac{\widetilde{Q^2}}{Q_h^2}\right)^{n_h+1}},$

$$L_s=\ln\left(\frac{s}{s_{0s}}\right),\quad \mathfrak{g}_{\mathfrak{s}}=2\left(\frac{a_s}{\widetilde{Q^2}}+\frac{b_s}{2m_p^2}\right),\quad \alpha_s(t)=\alpha_{0s}+\alpha'_st,$$
$$L_h=\ln\left(\frac{s}{s_{0h}}\right),\quad \mathfrak{g}_{\mathfrak{h}}=2\left(\frac{a_h}{\widetilde{Q^2}}+\frac{b_h}{2m_p^2}\right),\quad \alpha_h(t)=\alpha_{0h}+\alpha'_ht.$$
$$\mathfrak{B}=L_s\alpha'_s+L_h\alpha'_h+(\mathfrak{g}_{\mathfrak{s}}+\mathfrak{g}_{\mathfrak{h}}),\quad \mathfrak{L}=\frac{\pi}{2}(\alpha'_s-\alpha'_h),\quad \phi_0=\frac{\pi}{2}(\alpha_{0s}-\alpha_{0h}).$$
$$DL\quad pomerons:\quad \alpha_s(t)=1.08+0.25t,\quad \alpha_h(t)=1.44+0.01t.$$

2.3 Fitting results

Experimental data for the fits are taken from ISR, SPS experiments see.[2] for elastic *pp* scattering, and from ZEUS and H1 experiments [8, 9, 10, 11, 12, 13, 14, 15, 16, 18, 19, 20, 21] for vector meson production.

Our Preliminary fit results a listed in Table 1. The parameters without errors was fixed at fitting stage. We use only first term of eq. 10, i.e. A_h was fixed and equal to 0, and only half of all parameters were determined. Parameter n_s was set to be equal 0 for *pp* reaction, since there are no dependence in Q^2, and thus parameter $\widetilde{Q_s^2}$ can't be determined for this case. In future we hope to combine all the data and make single fit for all reaction.

	A_s	$\widetilde{Q_s^2}$	n_s	α_{0s}	α'_s	a_s	b_s	$\tilde{\chi}^2$
pp	5.9±5.7	$***$	0.00	1.05±0.14	0.28±0.47	2.88±2.84	0.00	1.52
ρ^0	59±29	1.33	1.35±0.05	1.15±0.06	0.15	-0.22	1.69	6.56
ϕ	32±35	1.30	1.32±0.10	1.14±0.12	0.15	-0.85±1.60	2.5±2.7	3.81
J/ψ	34±19	1.4 ±0.7	1.39±0.13	1.21±0.05	0.09	1.90	1.03	4.50
Υ(1S)	37±101	0.9 ±1.7	1.53±0.55	1.29±0.26	0.01±0.6	1.90	1.03	1.28
DVCS	9.7±9.0	0.45±0.5	0.94±0.24	1.19±0.09	-7e-3±0.3	1.94±4.65	1.7±2.3	1.75

Table 1: Fitting results.

2.4 pp elastic scattering

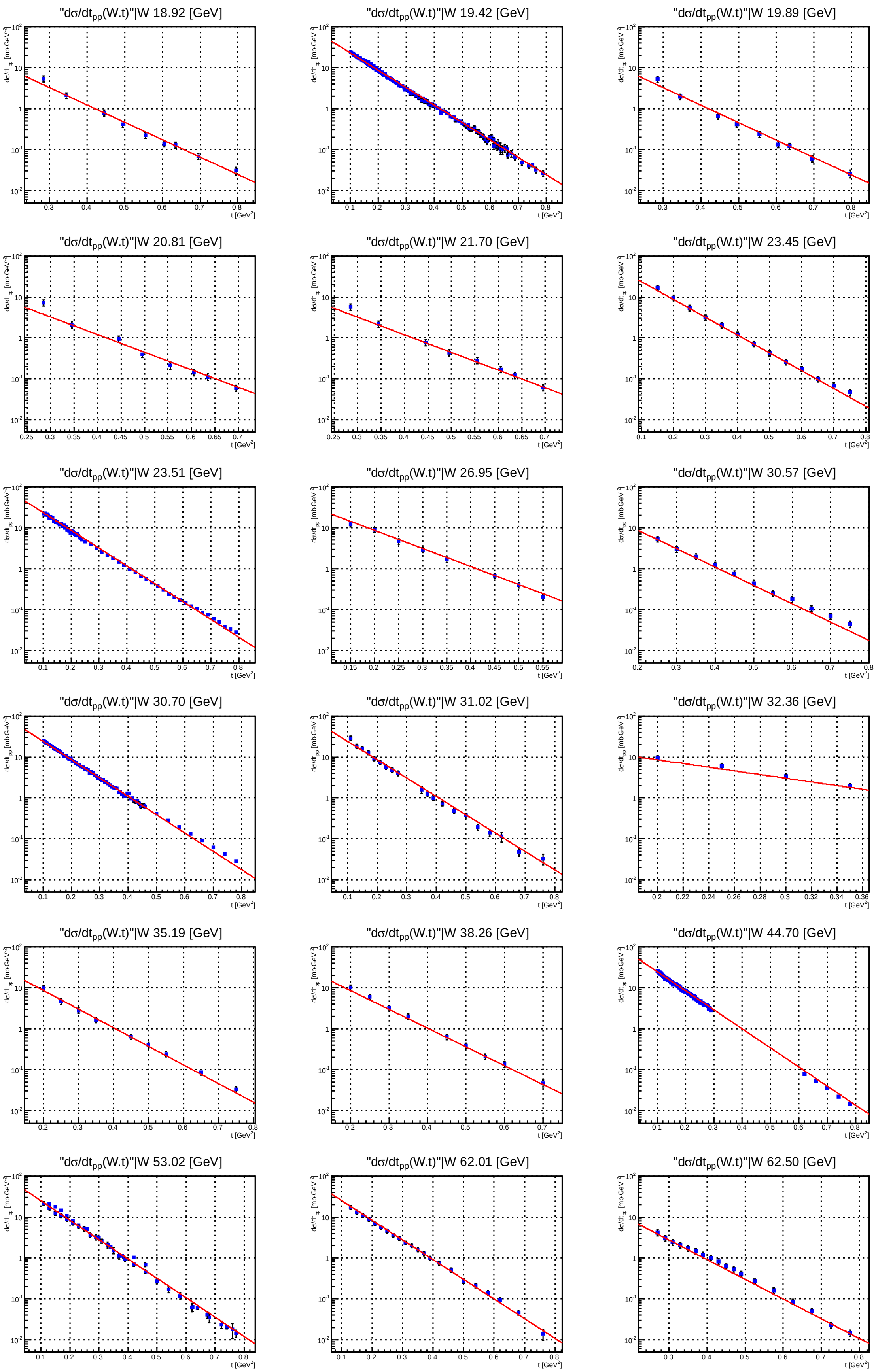

Figure 3: Differential cross sections for elastic pp scattering. Data form [7].

2.5 ρ^0 production

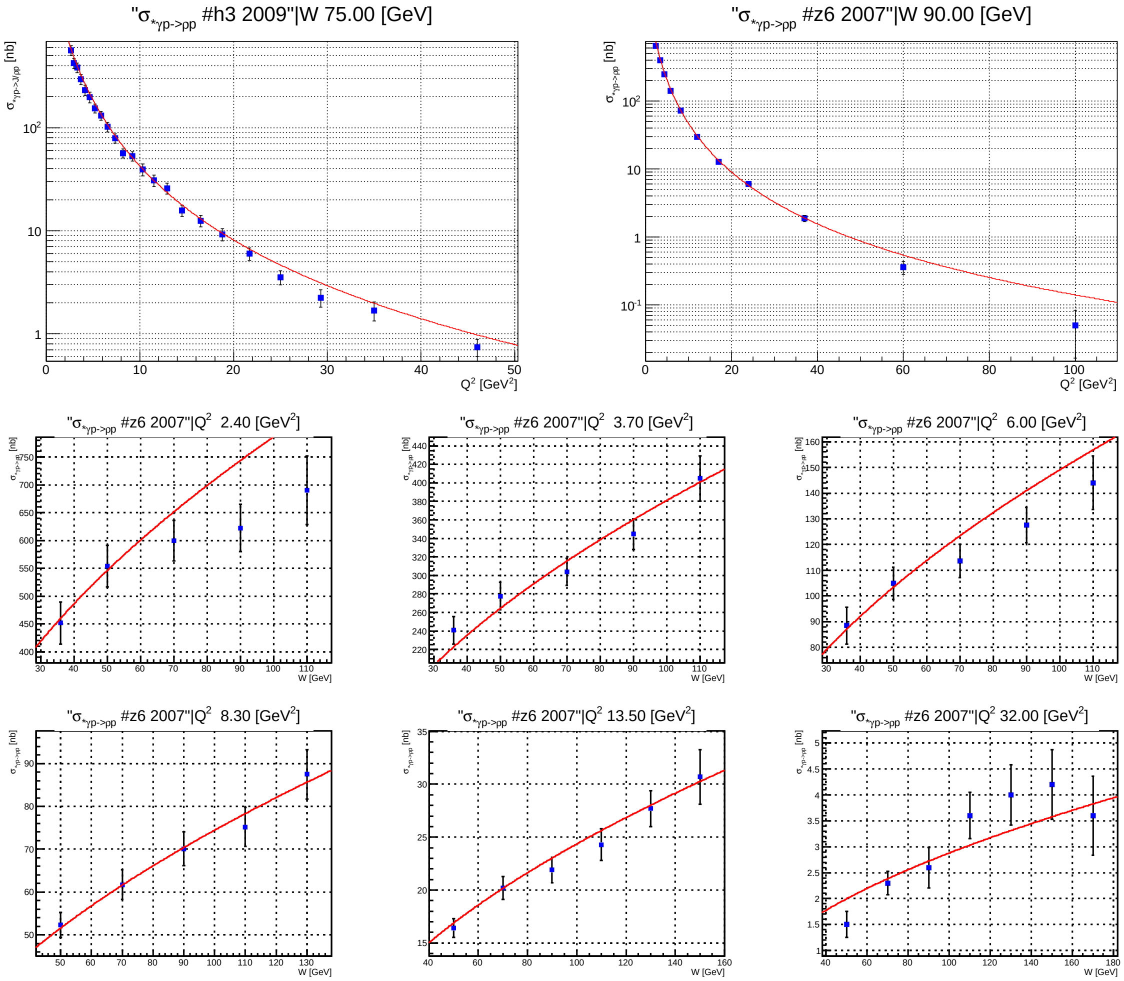

Figure 4: Integrated cross sections for ρ^0 production, [8, 9].

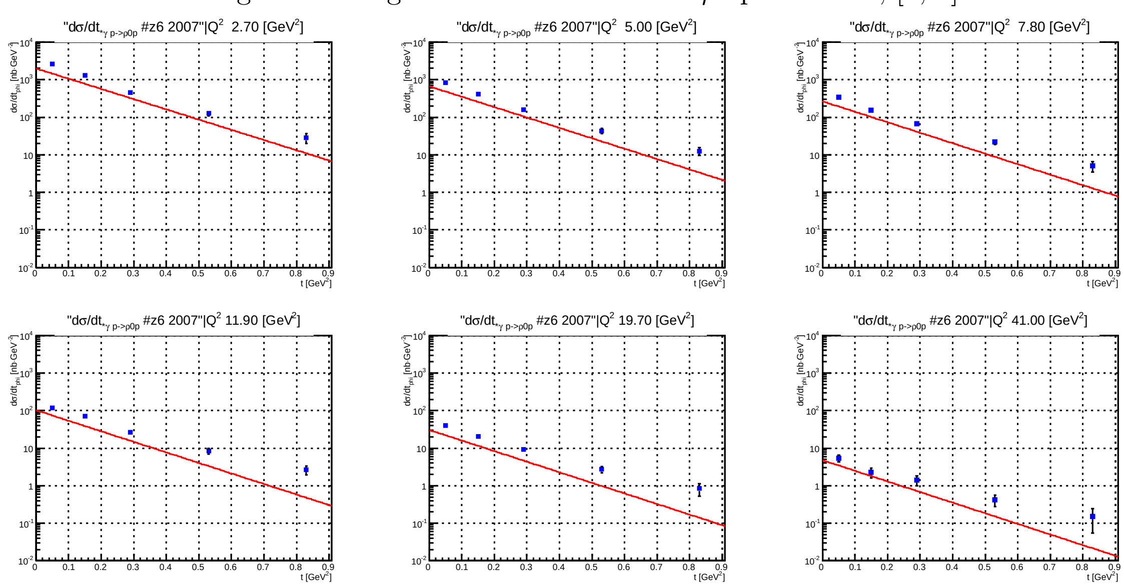

Figure 5: Differential cross sections for ρ^0 production. Data form [9].

2.6 ϕ production

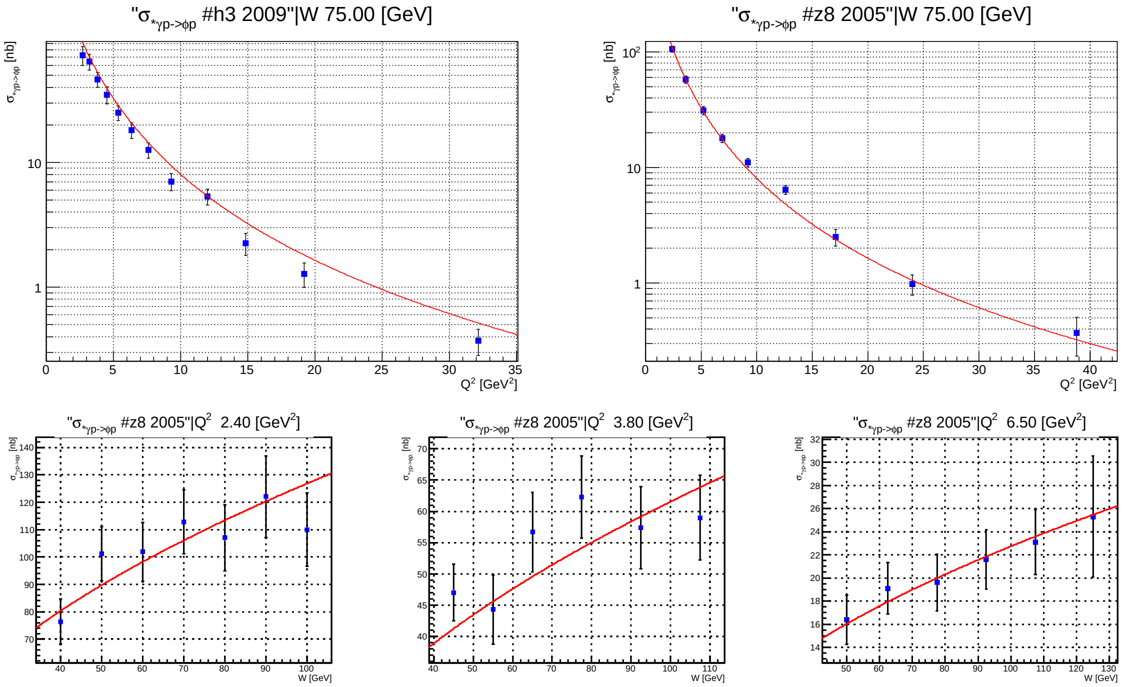

Figure 6: Integrated cross sections for ϕ production. Data form [8, 11].

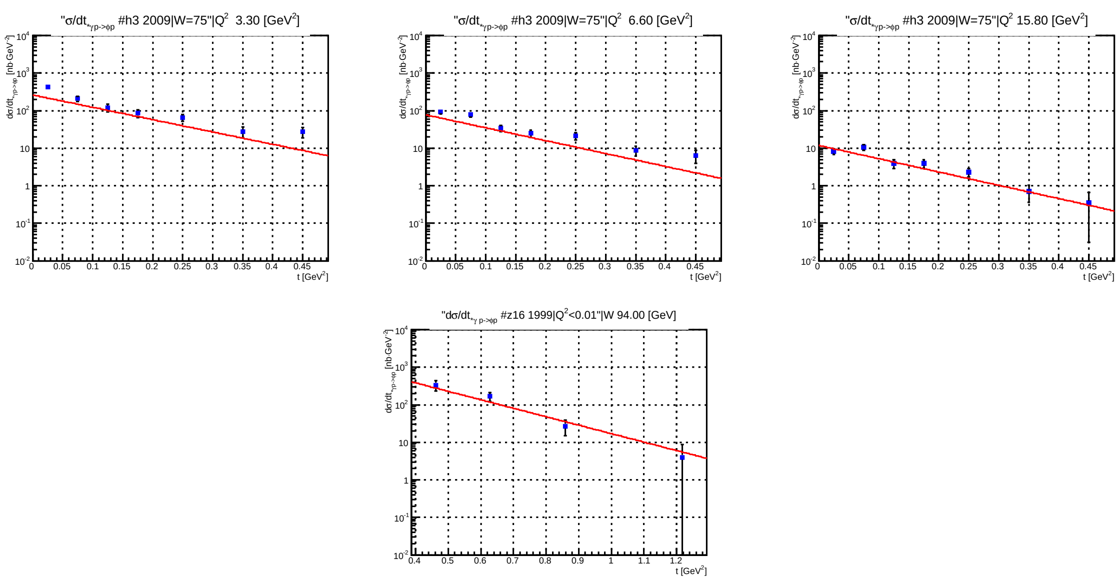

Figure 7: Differential cross sections for ϕ production. Data form [8, 10].

2.7 J/ψ production

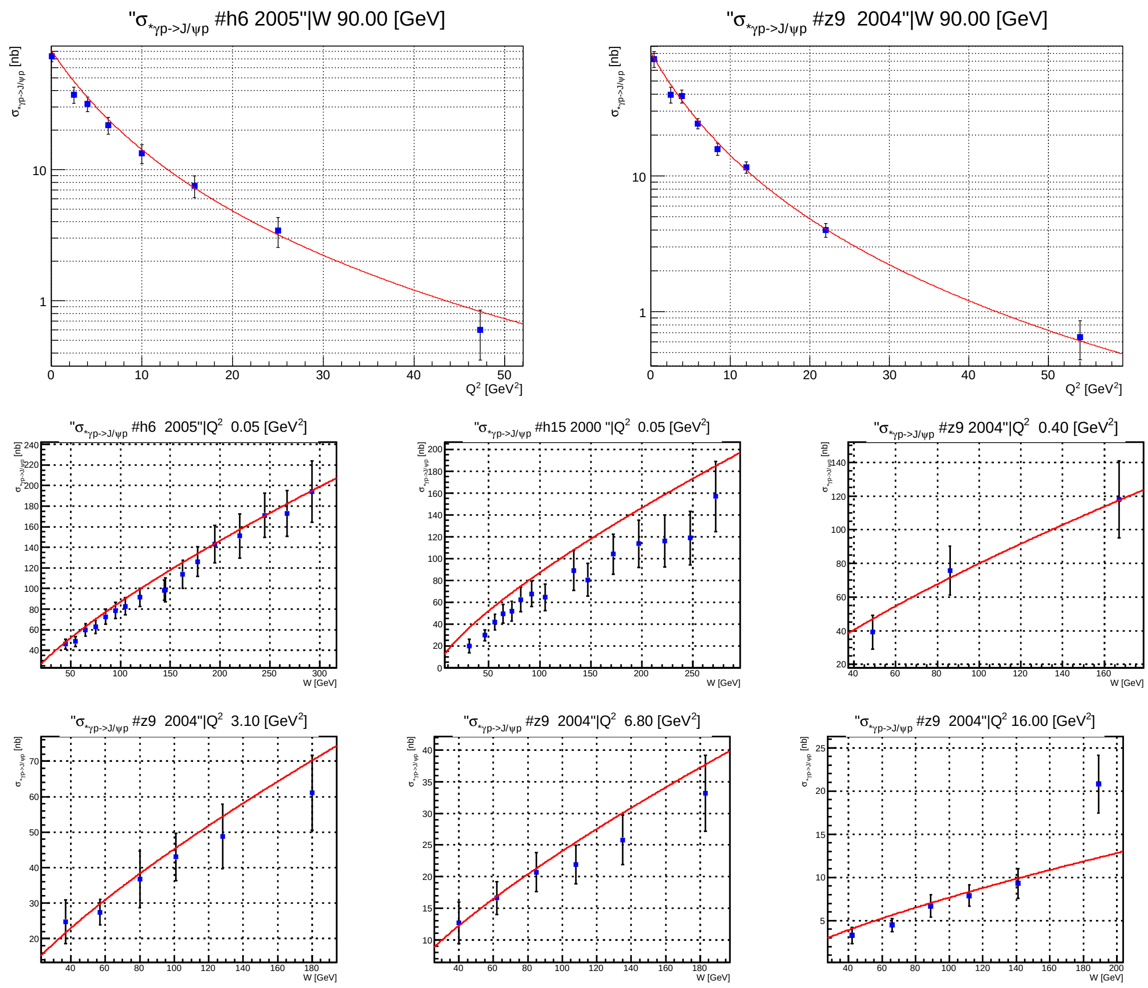

Figure 8: Integrated cross sections for J/ψ production. Data form [12, 13, 14].

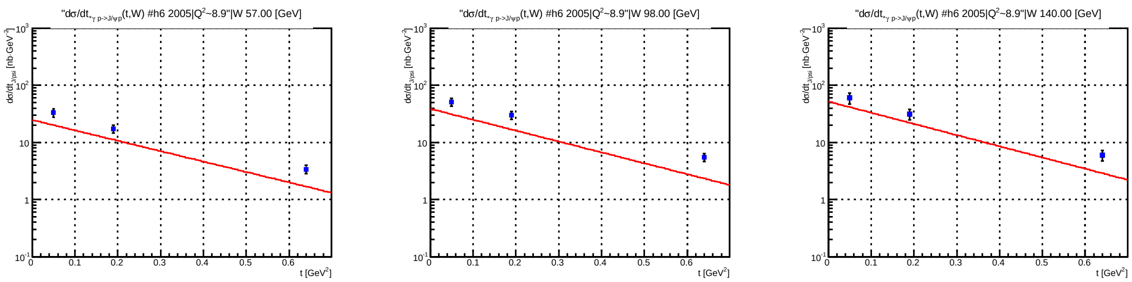

Figure 9: Differential cross sections for J/ψ electroproduction, H1 2005 form [12].

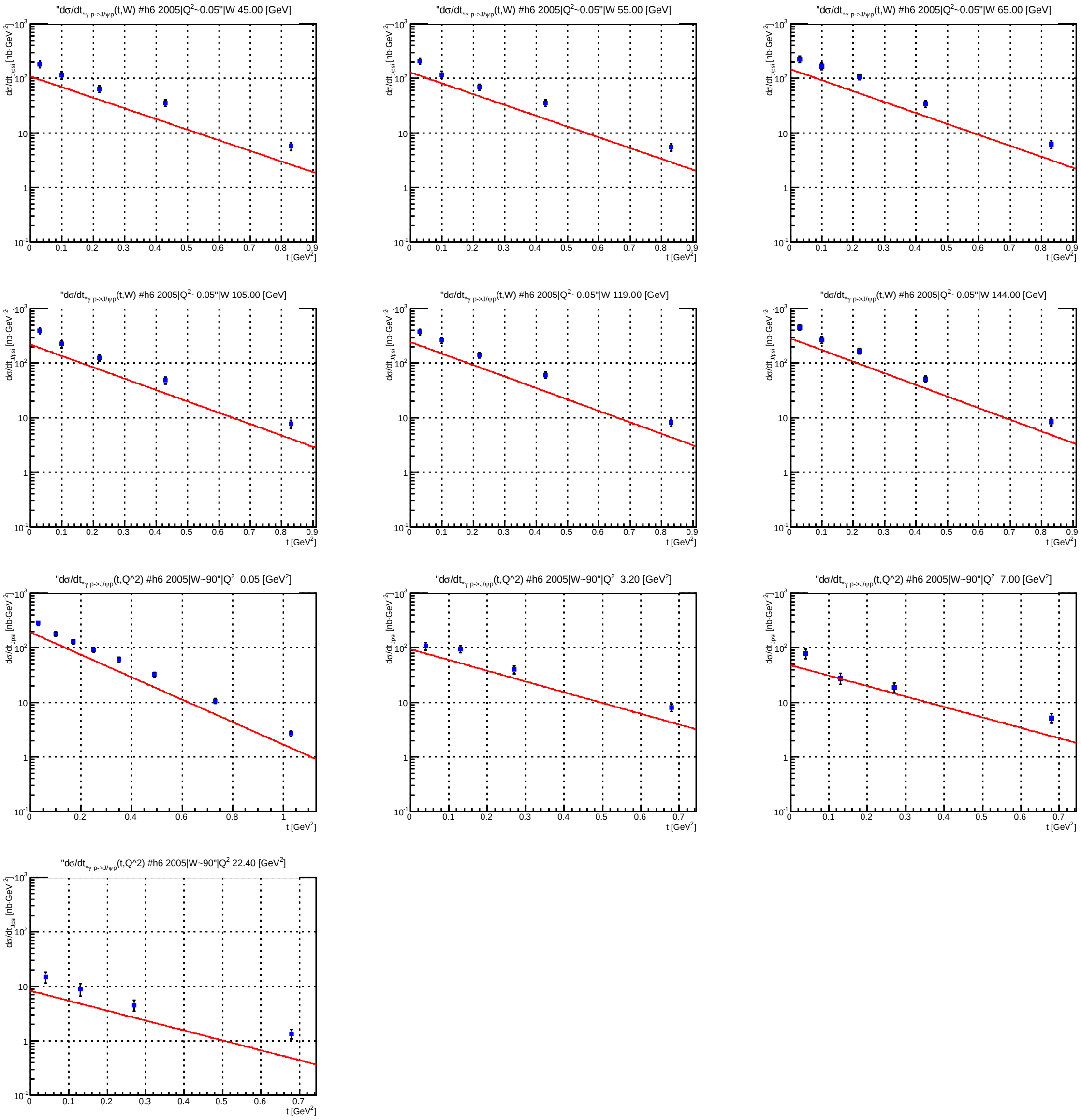

Figure 10: Differential cross sections for J/ψ electroproduction, H1 2005 from [12].

2.8 Υ production

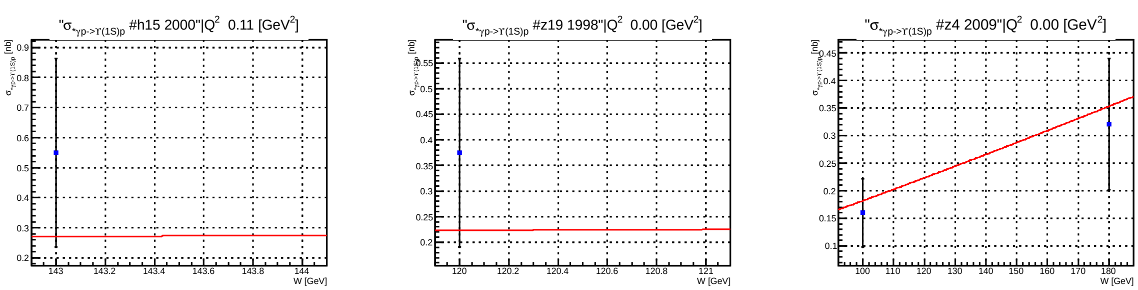

Figure 11: Integrated cross sections for $\Upsilon(1S)$ photoproduction. Data from [13, 15, 16].

2.9 DVCS

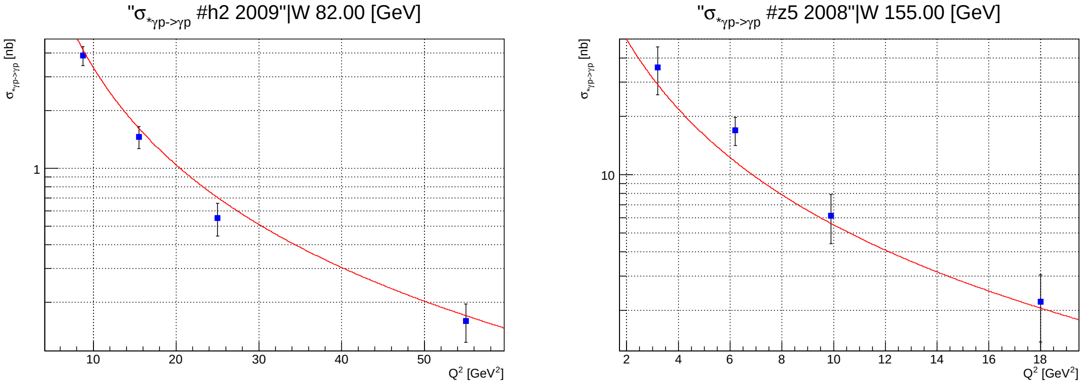

Figure 12: $\sigma(Q^2)$ DVCS. Data from [2, 18].

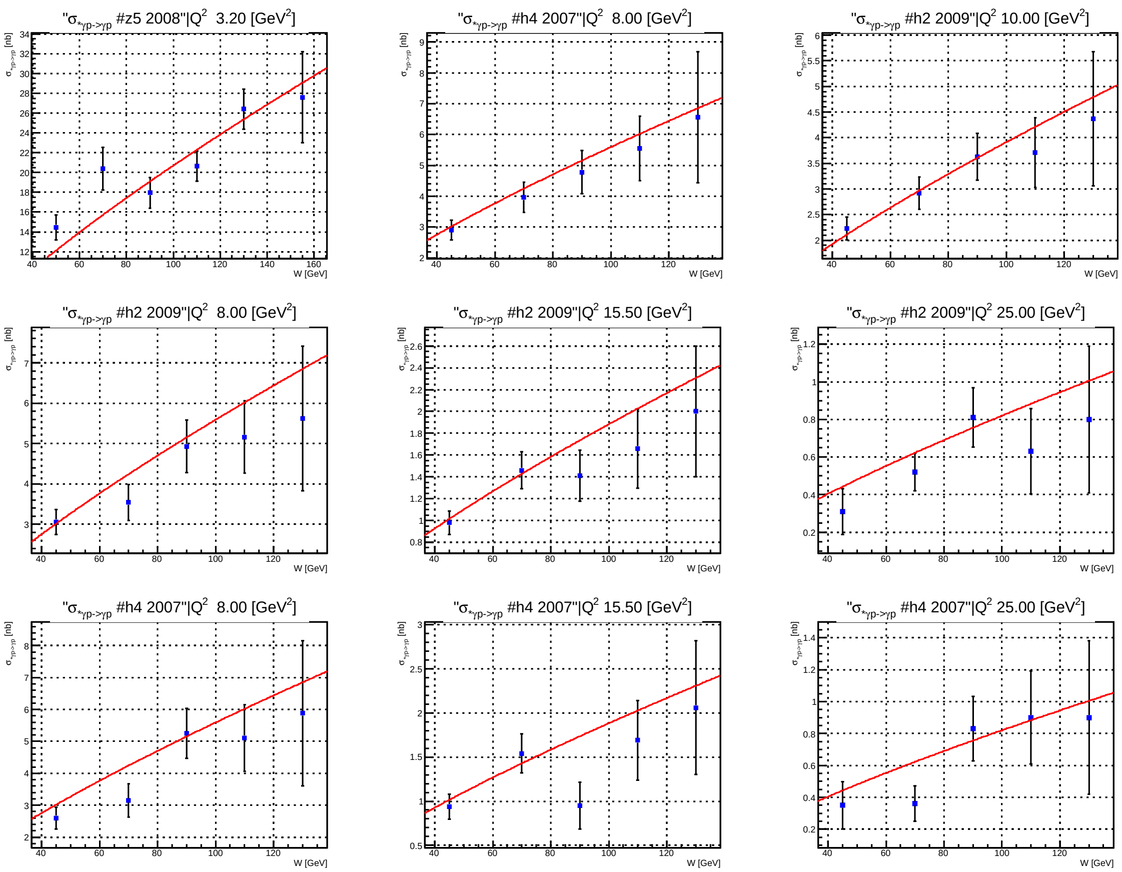

Figure 13: $\sigma(W)$ DVCS. Data from [2, 18, 19].

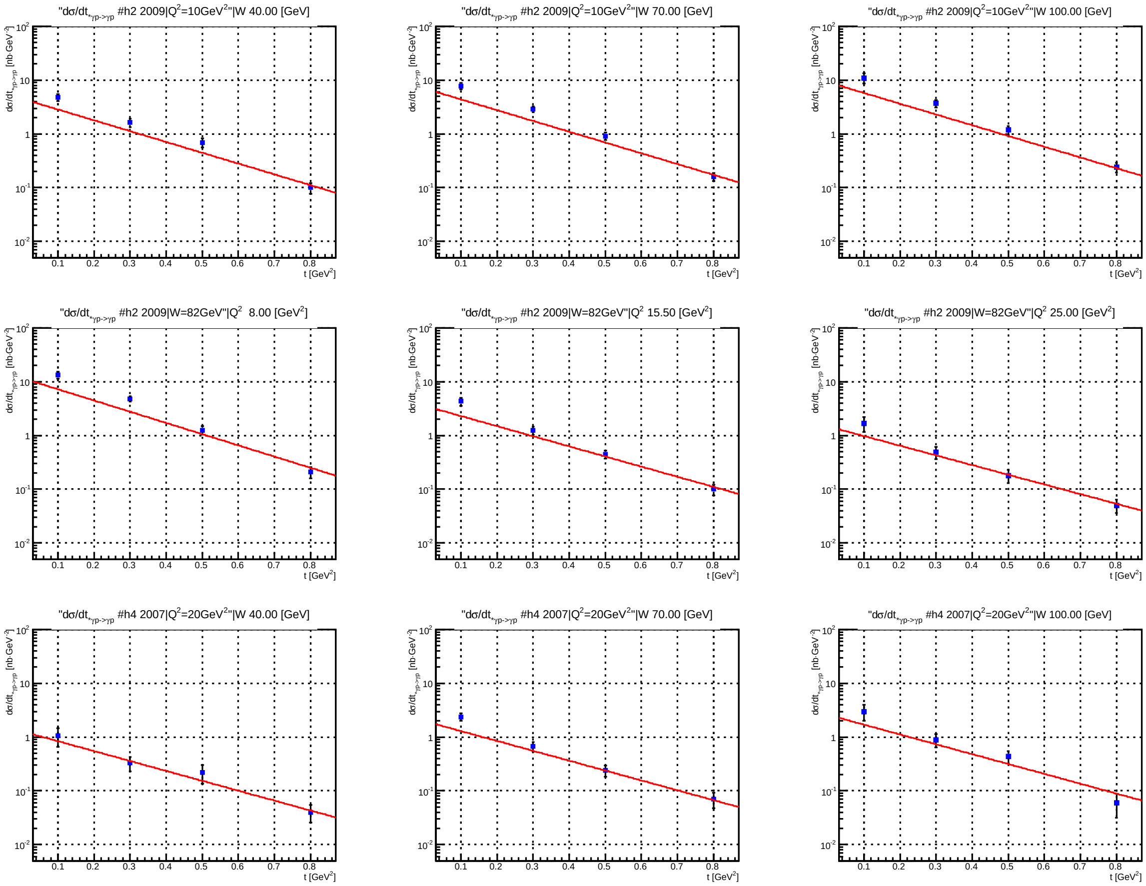

Figure 14: $\frac{d\sigma_{el}}{d|t|}$ DVCS. Data from [18, 19].

Acknowledgments

L. J. is grateful to the Organizers for the invitation and for the creative atmosphere during this Conference.

References

[1] R.Fiore, L.L. Jenkovszky and F. Paccanoni, Phys. Rev. D; [hep-ph/9812458].

[2] ZEUS Coll., S. Chekanov et al., JHEP **0905** (2009) 108, DESY 08-132, arXiv:0812.2517 [hep-ex].

[3] P. Landshoff, [hep-ph/0903.1523].

[4] A. Donnachie, P.V. Landshoff, [hep-ph/0803.0686].

[5] M. Capua, R. Fiore, S. Fazio, L. Jenkovszky, and F. Paccanoni, Phys. Lett. B **645** (2007) 161; [hep-ph/0605319].

[6] S. Fazio, R. Fiore, L.L. Jenkovszky and A.A. Lavorini , Phys. Rev **C 85**, 5 (2012).

[7] J.R. Cudell, A. Lengyel and E. Martynov, C Phys. Rev. **D73**: 034008, (2006) [arXiv:hep-ph/0511073].

[8] H1 Coll., F.D. Aaron et al., JHEP **1005** (2010) 032, DESY-09-093, arXiv:0910.5831[hep-ex].

[9] ZEUS Coll., S. Chekanov et al., PMC Phys. **A1** (2007) 6, DESY 07-118, arXiv:0708.1478 [hep-ex].

[10] ZEUS Coll., J. Breitweg et al., Eur.Phys.J.**C14** (2000) 213-238, DESY 99-160, [hep-ex/9910038].

[11] ZEUS Coll., S. Chekanov et al., Nuclear Physics **B718** (2005) 3-31, DESY-05-038, [hep-ex/0504010].

[12] H1 Coll., A. Aktas et al., Eur. Phys. J. **C46** (2006) 585-603, DESY-05-161,[hep-ex/0510016].

[13] H1 Coll., C. Adloff et al., Phys. Lett. **B483** (2000) 23-35, DESY-00-037, [hep-ex/0003020].

[14] ZEUS Coll., S. Chekanov et al., Nuclear Physics **B695** (2004) 3-37, DESY-04-052, [hep-ex/0404008].

[15] ZEUS Coll., S. Chekanov et al., Phys. Lett. **B680** (2009) 4-12, DESY-09-036, [hep-ex/0205107].

[16] ZEUS Coll., J. Breitweg et al., Physics Letters **B437** (1998) 432-444, DESY-98-089, [arXiv:hep-ex/9807020].

[17] ZEUS Coll., S. Chekanov et al., Physics Letters **B573** (2003) 46-62, DESY-03-059, [arXiv:hep-ex/0305028].

[18] H1 Coll., F. D. Aaron et al., Phys. Lett. **B681** (2009) 391, DESY 09-109, arXiv:0907.5289 [hep-ex].

[19] H1 Coll., A. Atkas et al., Phys.Lett. **B659** (2008) 796-806, DESY-07-142, arXiv:0709.4114 [hep-ex].

[20] H1 Coll., A. Atkas et al., Eur. Phys. J. **C44** (2005) 1-11, DESY-05-065, [hep-ex/0505061].

[21] H1 Coll., C. Adloff et al., Phys.Lett. **B517** (2001) 47,DESY-01-093, [hep-ex/0107005].